

# How target waves emerge in population dynamics with cyclical interactions

Luo-Luo Jiang<sup>1</sup>, Tao Zhou<sup>1,2</sup>, Xin Huang<sup>3</sup>, Bing-Hong Wang<sup>1</sup>

<sup>1</sup> Department of Modern Physics, University of Science and Technology of China, Hefei 230026, PR China

<sup>2</sup> Department of Physics, University of Fribourg, Chemin du Muse 3, CH-1700 Fribourg, Switzerland

<sup>3</sup> Department of Physics, University of Science and Technology of China, Hefei 230026, PR China

E-mail: bhwang@ustc.edu.cn

**Abstract.** Based on a multi-agent model, we investigate how target waves emerge from a population dynamics with cyclical interactions among three species. We show that the periodically injecting source in a small central area can generate target waves in a two-dimensional lattice system. By detecting the temporal period of species' concentration at the central area, three modes of target waves can be distinguished. Those different modes result from the competition between local and global oscillations induced by cyclical interactions: *Mode A* corresponds to a synchronization of local and global oscillations, *Mode B* results from an intermittent synchronization, and *Mode C* corresponds to the case when the frequency of the local oscillation is much higher than that of the global oscillation. This work provides insights into pattern formation in biologic and ecologic systems that are totally different from the extensively studied diffusion systems driven by chemical reactions.

PACS numbers: 87.23.Cc, 05.10.Ln, 87.18.Hf

## 1. Introduction

Spatially distributed excitable systems are widely investigated owing to their biological significance of long-range signal transmission through self-sustained waves [1, 2, 3, 4, 5, 6]. Pattern formation of wave propagation in excitable systems have been well studied [7]. Especially, target waves induced by noise have been found in the recurrent single species' population dynamics [6]. However, the formation mechanism of target waves in populations dynamics driven by multi-species' competitive interactions are not very clear.

Competitive interactions in natural and social systems consisted of many elements (e.g., various biological species, political parties, businesses, coupled reaction chemical components, bacterial production bacteria, etc.) play an important role in evolutionary processes and pattern formations [8, 9, 10, 11, 12, 13], and lead to the emergence of spatial patterns. In particular, target waves are commonly observed in those systems [14, 15, 16, 17, 18]. Previous works reveal that patterns could emerge in reaction-diffusion systems if one of the substances diffuses much faster than others [19, 20, 21]. For example, the bromous acid diffuses much faster than ferrion in the Belousov-Zhabotinsky (BZ) reaction and the cyclic AMP diffuses much faster than membrane receptor in the dictyostelium discoideum. However, many pattern formations of mobile population in ecosystems, such as migrating animals and running bacteria, can not be explained by the reaction-diffusion mechanism, since the diffusion speed induced by individual mobility is the same for all substances [22, 23]. Furthermore, partial differential equations (PDEs) have been proposed to describe the evolution of pattern formation in reaction-diffusion systems, such as the Oregonator model for BZ reaction [24]. Based on those PDEs, one can analyze the stability of patterns by using the mean field theory, but the reliable detailed information is quite limited. Therefore, it is necessary to use an agent-based models to describe the pattern formation of mobile population [11].

The cyclic predator-prey model provides a terse description of competition among population of different species. Experimental study [22] has revealed that the mechanism of rock-paper-scissors game can promote the biodiversity of three strains of *Escherichia coli*. Very recently, Reichenbach *et al* proposed a rock-paper-scissors game of mobile populations [8], where the individual mobility displays a critical effect on species diversity. When mobility is below a certain value, all species coexist and form spiral waves. In contrast, above this threshold biodiversity is jeopardized. Indeed, previous investigations show that the cyclical competition mechanism and low mobility of individuals maintain the biodiversity in ecosystems [8, 25, 22, 26, 27]. In this paper, we investigate the pattern formation based on a cyclic predator-prey model with mobile individuals. Target waves are observed from the recurrent dynamics driven by three species' competitive interactions. As a result of global oscillation, a transition from disordered state to an ordered spacial structure occurs with the increasing of injection period in the vortex of target waves. By detecting the temporal period of species' concentration at the central area, three modes of target waves can be distinguished.

Those different modes result from the competition between local and global oscillations induced by cyclical interactions: *Mode A* corresponds to a synchronization of local and global oscillations, *Mode B* results from an intermittent synchronization, and *Mode C* corresponds to the case when the frequency of the local oscillation is much higher than that of the global oscillation. Though the present model only concerns the microscopic interactions among individuals, target waves emerge in a macroscopic level. Furthermore, our work provides a feasible method for pattern control and pattern selection.

## 2. Stochastic cyclic predator-prey model

Based on the previous works of Reichenbach *et al* [8, 25], we introduce a cyclic predator-prey model as follow: Mobile individuals of three species (marked by 1, 2, 3) locate in the nodes of a two-dimensional regular lattice with no flux boundary. Here a node stands for an  $1 \times 1$  square. Each node can be occupied by at most one individual of a species or a vacancy (denoted by  $V$ ) representing resource. There are three kinds of interactions, namely exchange, predation, and reproduction, which only occur between neighboring nodes. *Exchange*.— An individual could exchange positions with one of its neighbors at a rate  $\alpha$  due to its mobility. *Predation*.— 1 beats 2 and 2 becomes a vacancy at a predation intensity  $\beta$ , in the same way, 2 beats 3, and 3 beats 1. *Reproduction*.— An individual can reproduce an offspring to a neighboring  $V$  node at a rate  $\gamma$ .

Unlike the deterministic approach which regards the time evolution as a continuous process, here, the applied stochastic approach regards the time evolution as a kind of random-walk process. In this model, reactions occur in a random manner: exchange happens with probability  $\alpha/(\alpha + \beta + \gamma)$ , predation with probability  $\beta/(\alpha + \beta + \gamma)$ , and reproduction with probability  $\gamma/(\alpha + \beta + \gamma)$ . We use a standard algorithm for stochastic simulation, which was developed by Gillespie [28, 29].

## 3. Results

Inspired by the experiments of growth of *Escherichia coli* on a petri dish [15], we apply the dynamical model of three populations' cyclical interactions [8]. In an  $L \times L$  lattice, each node presents a space occupied by a vacancy or an individual of a species, and at each time step a randomly chosen individual interacts with one of its four nearest neighbors, which is also determined randomly according to the corresponding predation intensity. The evolving process is implemented by using the Gillespie algorithm [28, 29] in which one Monte Carlo (MC) time is defined as the time period during which all the individuals have been chosen once on average. Hereinafter, the resolution of time is defined as one MC time. Initially, the lattice is wholly occupied by vacancies, and then populations of a species are injected periodically in a central area, namely the *injected area*. An illustration of the injected area is shown in Fig. 1. In this paper, the injected radius,  $R$ , is set as 10.5 and the lattice size,  $L$ , is 1024. The injected species revolve in

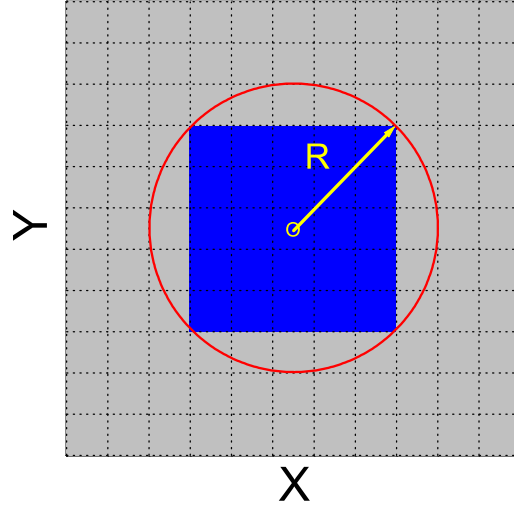


**Figure 1.** Illustration of the injected area in an  $11 \times 11$  lattice. Here,  $R$  is set as 3.5, and the lattice completely inside the circle, marked by the blue color, is the injected area. In the simulation of this paper, the injected radius  $R$  is fixed as 10.5.

the order 1, 2, 3, 1, 2, 3, ... For example, populations of 1 are injected at  $t = 0$ , then 2 at  $t = T_0$ , 3 at  $t = 2T_0$ , and 1 at  $t = 3T_0$ , etc. In this case, the period of injecting is  $T_{in} = 3T_0$ , where  $T_0$  is the interval time between injections of two species.

Mobility is an important character for most population dynamics such as bacteria swimming and tumbling. The mobility in the present model corresponds to the action that an individual moves to a neighboring empty node ( $V$  node), which is defined as:

$$M = 2\alpha/N, \quad (1)$$

where  $N = L^2$  is the number of nodes in the system. In this paper,  $L = 1024$ ,  $\beta = 1$  and  $\gamma = 1$  are fixed.

With no-flux boundary conditions, extensive computer simulations are performed and the system displays abundance phenomena of pattern formation with various injection periods. In order to describe the spatial structure of pattern formation, we define  $\rho = N_0/N$ , where  $N_0$  is the number of individuals in the largest *adjacent population*. Here, an adjacent population is a set of individuals of one species where any two individuals can be connected through a sequence of nearest neighboring relations within this set. Apparently, patterns break when  $\rho$  approaches to 0, while one species occupies the whole system when  $\rho$  reaches 1. As shown in Fig. 2(d), given  $M = 10^{-5}$ , with the increasing of  $T_0$ , the system undergoes a transition from a state of coexistence of three species to a state occupied by one species. The pattern formations corresponding to the points  $a$ ,  $b$ , and  $c$  in Fig. 2(d) are shown in Fig. 2(a), 2(b), and 2(c) respectively. When  $T_0$  is small ( $T_0 \leq 300$ ) the three species form many small spiral waves which can be

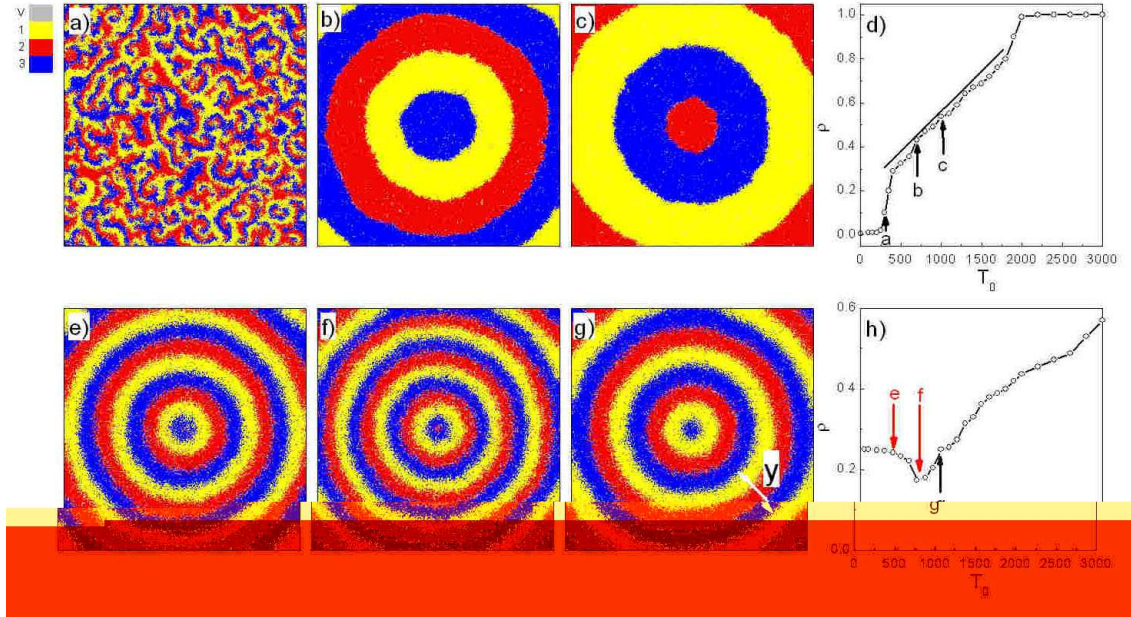


**Figure 2.** The panels (a), (b), (c), (e), (f) and (g) display different pattern formations generated in the present model. The panels (d) and (h) report  $\rho$  as a function of  $T_0$ . (a), (b), (c), (d) for  $M = 10^{-5}$  and (e), (f), (g), (h) for  $M = 10^{-4}$ . (a) and (e) for  $T_0 = 300$ , (b) and (f) for  $T_0 = 500$ , (c) and (g) for  $T_0 = 1000$ . The cases presented in (a), (b), and (c) are marked by  $a$ ,  $b$ , and  $c$  in (d), and the cases presented in (e), (f), and (g) are marked by  $e$ ,  $f$ , and  $g$  in (h). In (d), the relation  $\rho(T_0)$  can be approximately linearly fitted in the interval  $T_0 \in (500, 1800)$ . In (g),  $y$  denotes the spatial distance between neighboring wave fronts for the same species.

considered as a disordered state in global level. Fig. 2(b) and Fig. 2(c) show target waves emerging for  $T_0 = 500$  and  $T_0 = 1000$ . The system becomes more and more ordered, reaches a consensus state when  $T_0 \geq 2000$ . In contrast, for  $M = 10^{-4}$ , Fig. 2(h) shows an unexpected decline with the increasing of  $T_0$ , and the pattern formations corresponding to the points  $e$ ,  $f$ ,  $g$ , are shown in Fig. 2(e), 2(f), and 2(g), respectively.

It is worth mentioning that all patterns in our results are robust after the systems have reached steady states. It seems that target waves emerge because of the increasing of  $T_{in}$ . A question is naturally taken into consideration: How  $T_{in}$  affects the pattern formation. Furthermore, one may ask why  $\rho$  is monotonously increasing with the increasing of  $T_0$  in Fig. 2(d), while non-monotonously varying in Fig. 2(h). We calculate the proportion of species 1 in the injected area. With  $T_0 = 600$ , this proportion does not display periodicity for  $M = 10^{-6}$  (see Fig. 3(a)), while varies periodically for  $M = 10^{-5}$  (see Fig. 3(b)) as well as for  $M = 10^{-3}$  (see Fig. 3(d)), and shows quasi-periodical behavior for  $M = 10^{-4}$  (see Fig. 3(c)). The period is  $T = 2T_{in} = 3600$  for  $M = 10^{-5}$ , and  $T = T_{in} = 1800$  for  $M = 10^{-3}$ . Fig. 3(e), 3(f), 3(g), and 3(h) show (the varying of) three species' proportions in the whole system one-to-one corresponding to the evolving processes of Fig. 3(a), 3(b), 3(c), and 3(d). Clearly, Fig. 3(a)-3(d) show the local

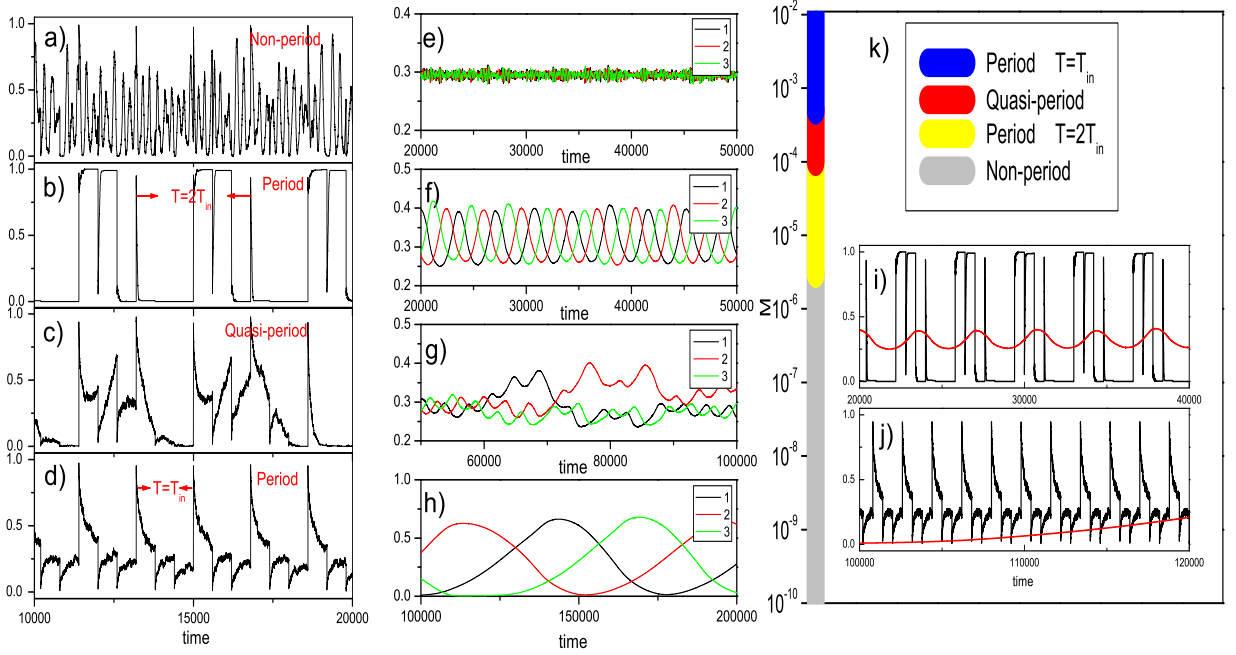


**Figure 3.** The panels (a)-(d) report the proportion of species 1 in the injected area for different mobilities, while (e)-(h) display proportions of three species in the whole system. Panels (e)-(h) are one-to-one corresponding to panels (a)-(d).  $T_0$  is fixed as 600,  $M = 10^{-6}$  for (a) and (c),  $M = 10^{-5}$  for (b) and (f),  $M = 10^{-4}$  for (c) and (g),  $M = 10^{-3}$  for (d) and (h). The panel (k) shows different system states from  $M = 10^{-10}$  to  $M = 10^{-2}$ , given  $T_0 = 600$ . The insets (i) and (j) display the comparison of species 1's proportions in the injected area (black) and the whole system (red), (i) for  $M = 10^{-5}$  (corresponding to (b) and (f)) and (j) for  $M = 10^{-3}$  (corresponding to (d) and (h)).

oscillations in the injected area, while Fig. 3(e)-3(h) display the global oscillations. Fig. 3(i) and Fig. 3(j), corresponding to the cases shown in 3(b) and 3(d), compared the local and global oscillations of species 1. In Fig. 3(i), the local and global oscillations have the same period, while in Fig. 3(j), the frequency of the local oscillation is much higher than that of the global oscillation. We say, in the case shown in Fig. 3(b), 3(f) and 3(i), the local and global oscillations are synchronous at  $T = 2T_{in}$ , while in the case shown in Fig. 3(d), 3(h) and 3(j), they are non-synchronous. In between, the system displays quasi-periodical behavior, and the local and global oscillations are intermittent synchronous (see, for example, Fig. 3(c) and 3(g)). According to the above discussion, a qualitative classification of system states versus mobility is shown in Fig. 3(k), including non-period, period  $T = 2T_{in}$ , quasi-period, and period  $T = T_{in}$ .



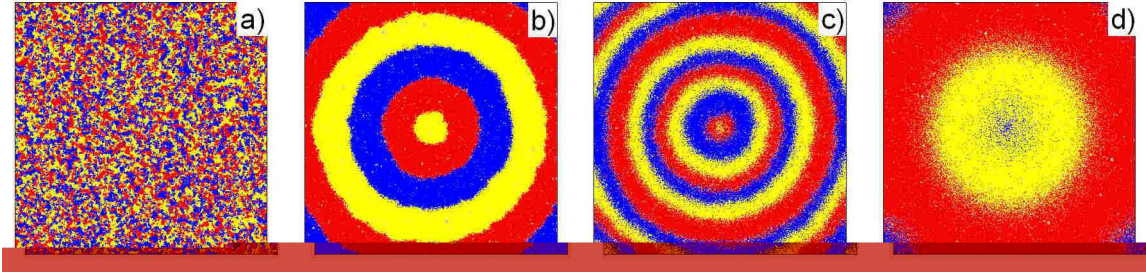


**Figure 4.** The panels (a)-(d) show pattern formations corresponding to the cases shown in Fig. 3(a), (b), (c), and (d) respectively.

As shown in Fig. 4, there are four qualitatively different states, and the patterns in Fig. 4(b), Fig. 4(c) and Fig. 4(d) are named as *Mode A*, *Mode B* and *Mode C*. When a species is injected, individuals of this species will interact with other species around.

(i) For extremely small value of  $M$  ( $< 3.0 \times 10^{-6}$ ), individuals out of the injected area distribute almost homogeneously due to a relatively high rate of predation and reproduction. The injected individuals, surrounded by other two species, are segmented into fragments. Therefore, as shown in Fig. 4(a) the local oscillations have no period, and no global ordered pattern formats.

(ii) For small value of  $M$  ( $< 10^{-4}$ ), individuals out of the injected area are inhomogeneously distributed due to a relatively low rate of predation and reproduction. The injected individuals are surrounded by only the prey species, and each species takes up the injected area for  $2T_{in}/3$ , thus the period of local oscillations is  $2T_{in}$ . The boundary between the two species near the injected area moves from the center to the whole system, inducing a global oscillation with period  $2T_{in}$  too. This case is shown in Fig. 4(b) and referred to as *Mode A*.

(iii) For medium value of  $M$  ( $10^{-4} < M < 5.0 \times 10^{-4}$ ), although individuals out of the injected area are inhomogeneously distributed due to a relatively low rate of predation and reproduction, the injected individuals are surrounded by all three species. No species takes up the whole injected area and the period of local oscillations is  $2T_{in}$  sometimes (see Fig. 3(c)). In other words, local oscillations are confined in the injected area sometimes. Therefore, the local oscillations is quasi-periodic and intermittently synchronized with the global oscillations. This case is shown in Fig. 4(c) and referred to as *Mode B*.

(iv) When  $M$  is sufficiently large ( $> 5.0 \times 10^{-4}$ ), the relative rate of predation and reproduction is very low. Three species coexist near the boundary of the injected area. Because the number of injected individuals is quickly depressed, no species dominates the whole injected area (see Fig. 3(d)). Local oscillations are confined in the injected area, and individuals of a species will aggregate near the boundary of the injected area, and then move from the center to the whole system. Since the aggregation and propagation takes a long time, the period of global oscillations is much longer than that of local oscillations. Target waves formatting in this manner are called *Mode C*.

The wavelength is defined as  $\lambda = y/L$ , where  $y$  is denotes the spatial distance between neighboring wave fronts with the same species in the lattice as shown in

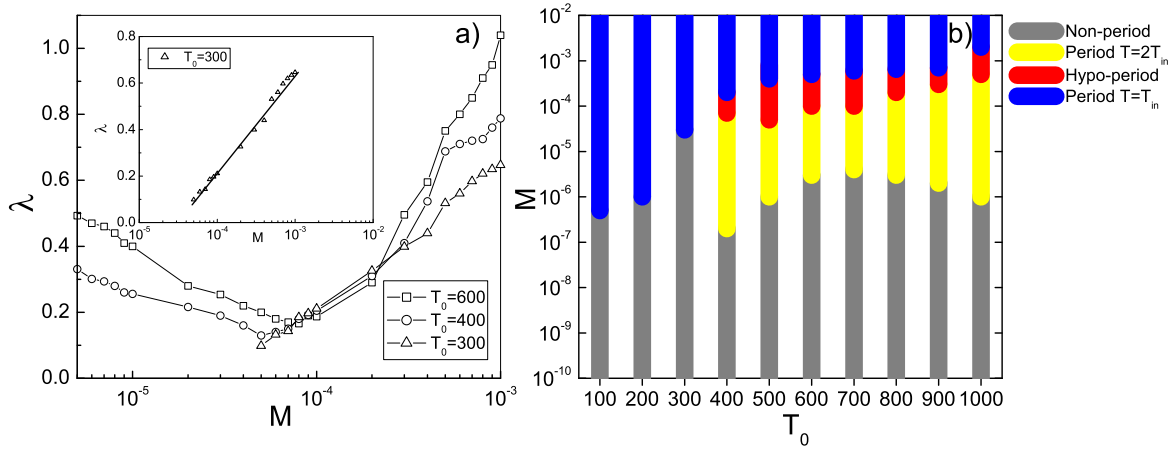


**Figure 5.** (a) Wavelength of target waves as a function of  $M$  for different values of injection period  $T_0$ . The inset shows  $\lambda \sim \log M^{1/2}$ . (b) Different system states in  $M - T_0$  space.

Fig. 2(g). Comparing Fig. 4(b), Fig. 4(c), and Fig. 4(d), one can find that wavelengths of target waves in both *Mode A* and *Mode C* are longer than that in *Mode B*, and wavelengths of target waves in *Mode B* are inequable. It can explain why Fig. 2(h) have a trop. The reason is target waves belong to *Mode B* for  $T_0 > 300$  and  $T_0 \leq 800$  at  $M = 10^{-4}$ , while others belong to *Mode A* or *Mode C*, and wavelengths of *Mode B* are smaller than that of *Mode A* and *Mode C*. Moreover, the target waves become unstable when  $T_0$  goes across the critical point distinguishing two different modes, and may evolve into spiral waves which is also observed in a system of a single species, *Dictyostelium* system [6, 30].

As shown in Fig. 5(a), wavelengths of target waves display non-monotonic behavior with the mobility of individuals for  $T_0 = 600$  and  $T_0 = 400$ , while increase with  $M$  in terms of  $\lambda \sim \log M^{1/2}$  for  $T_0 = 300$ . This phenomena are different from the cases of spiral waves [8], in which  $\lambda \sim M^{1/2}$ . The non-monotonic increasing with the mobility  $T_0 = 400$  and  $T_0 = 600$  is caused by the target waves of *Mode B* (see red blocks in Fig. 5(b)).

#### 4. Summary

Cyclical competition, an important principle of ecology and society, leads to complex phenomena of maintenance of ecological bio-diversity and emergence of cooperation in society, where spatial distribution of populations plays a critical role [31, 32, 33, 34]. It has been found that multi-species' competition induces complex spatiotemporal structures in ecological systems. Especially, the 3-species evolving game, namely rock-



paper-scissors game or cyclic predator-prey model, reveals spiral wave structures [35, 36]. However, target waves are rarely reported. In the current model, target waves emerge under a suitable initial condition, which is in accordance with the observations in real bacteria systems [6, 30]. Although target waves were also observed in many excitable media, in our model, individuals of three species move at the same rate, which distinguishes our model from the diffusion systems driven by chemical reactions where different substances have different moving speeds. Indeed, our results suggest that target waves can be driven by the competition of local and global oscillations. This newly reported mechanism could provide insights into target waves formation in biologic and ecologic systems.

In addition, our results can be applied in pattern control. Actually, the system makes stochastic resonance to the periodical injection fluid in *Mode A*, which can be used to control the global behaviors since the injection period is controllable. Recently, the periodic injection method is also used in complex Ginzburg-Landau system for the purpose of spatiotemporal chaos control [37, 38]. The periodical injection for pattern control has great significance in potential applications of toothful medication transportation.

## Acknowledgments

The authors would like to thank Dan Peng, Tian-Shuo Hu, Xiao-Pu Han, and Shi-Min Cai for their assistances in preparing this manuscript. This work is supported by the National Basic Research Program of China (973 Program No. 2006CB705500), the National Natural Science Foundation of China (Grant Nos. 10635040, 10532060 and 10472116), and by the Specialized Research Fund for the Doctoral Program of Higher Education of China.

## References

- [1] Kapral R and Showalter K eds 1995 *Chemical Waves and Patterns* (Kluwer, Dordrecht, The Netherlands)
- [2] Sammak P J, Hinman L E, Tran P O T, Sjaastad M D and Machen T E 1997 *J. Cell Sci.* **110** 165
- [3] Bootman M D, Lipp P and Berridge M J 2001 *J. Cell Sci.* **114** 2213
- [4] Přibyl M, Muratov C B and Shvartsman S Y 2003 *Biophys. J.* **84** 883
- [5] Weissman T A, Riquelme P A, Ivic L, Flint A C and Kriegstein A R 2004 *Neuron* **43** 647
- [6] Cyrill B M, Eric V-E and Weinan E 2007 *Proc. Natl. Acad. Sci. U. S. A.* **104** 702
- [7] Meron E 1992 *Phys. Rep.* **218** 1
- [8] Reichenbach T, Mobilia M and Frey E 2007 *Nature* **448** 1046
- [9] Perc M and Szolnoki A 2007 *New J. Phys.* **9** 267
- [10] Igoshin O A, Welch R, Kaiser D and Oster G 2004 *Proc. Natl. Acad. Sci. U. S. A.* **101** 4256
- [11] Carneiro M V and Charret I C 2007 *Phys. Rev. E* **76** 061902
- [12] Sinervo B, Heulin B, Surget-Groba Y, Clobert J, Miles D B, Corl A, Chainé A and Davis A 2007 *Am. Nat.* **170** 663
- [13] Mobilia M, Georgiev I T and Täuber U C 2006 *Phys. Rev. E* **73** 040903(R)

- [14] Zaikin A N and Zhabotinsky A M 1970 *Nature* **225** 535
- [15] Budrene E O and Berg H C 1995 *Nature* **376** 49
- [16] Pálsson E and Cox E C 1996 *Proc. Natl. Acad. Sci. U. S. A.* **93** 1151
- [17] Lee K J, Cox E C and Goldstein R E 1996 *Phys. Rev. Lett.* **76** 1174
- [18] Hendrey M, Nam K, Guzdar P and Ott E 2000 *Phys. Rev. E* **62** 7627
- [19] Turing A M 1952 *Philos. Trans. R. Soc. London Ser. B* **237** 37
- [20] Cross M C 1993 *Rev. Mod. Phys.* **65** 851
- [21] Koch A J and Meinhardt H 1994 *Rev. Mod. Phys.* **66** 1481
- [22] Kerr B, Riley M A, Feldman M W and Bohannon B J M 2002 *Nature* **418** 171
- [23] Kirkup B C and Riley M A 2004 *Nature* **428** 412
- [24] Field R J and Noyes R M 1974 *J. Phys. Chem.* **60** 1877
- [25] Reichenbach T, Mobilia M and Frey E 2007 *Phys. Rev. Lett.* **99** 238105
- [26] Reichenbach T, Mobilia M and Frey E *J. Theor. Biol.* (in press)
- [27] Nowak M A and Sigmund K 2002 *Nature* **418** 138
- [28] Gillespie D T 1976 *J. Comput. Phys.* **22** 403
- [29] Gillespie D T 1977 *J. Phys. Chem.* **81** 2340
- [30] Lee K J, Goldstein R E and Cox E C 2001 *Phys. Rev. Lett.* **87** 068101
- [31] Nowak M A, Bonhoeffer S and May R M 1994 *Proc. Natl. Acad. Sci. U. S. A.* **91** 4877
- [32] Nowak M A, Sasaki A, Taylor C and Fudenberg D 2004 *Nature* **428** 646
- [33] Nowak M A and Sigmund K 2004 *Science* **303** 793
- [34] Szabó G and Fáth G 2007 *Phys. Rep.* **446** 97
- [35] Szabó G, Santos M A and Mendes J F F 1999 *Phys. Rev. E* **60** 3776
- [36] Szolnoki A and Szabó G 2005 *Phys. Rev. E* **71** 027102
- [37] He X-Y, Zhang H, Hu B-B, Cao Z-J, Zheng B and Hu G 2007 *New J. Phys.* **9** 66
- [38] Jiang M-X, Wang X-N, Ouyang Q and Zhang H 2004 *Phys. Rev. E* **66** 056202